JOURNAL OF COMPUTATIONAL PHYSICS 37, 336–354 (1980)

# Subgrid Resolution of Fluid Discontinuities, II

J. GLIMM,*,† D. MARCHESIN,†,‡ AND O. MCBRYAN§,**

*The Rockefeller University, New York, New York 10021*

Received July 5, 1979; revised October 9, 1979

In computation of discontinuities in solutions of hyperbolic equations, the random choice method gives a zero viscosity numerical solution with perfect resolution but first-order position errors $\sim\pm 2.5\Delta x$. The Lax–Wendroff scheme gives very small first-order position errors, but resolution errors $\sim\pm 2.5\Delta x$. We propose two very simple tracking methods in the context of the random choice method, which combine the best features of both methods: perfect resolution and good accuracy. We compare the above with tracking in the context of the Lax–Wendroff scheme. The latter method is morre complicated, but much more accurate than any of the other methods considered here.

## 1. INTRODUCTION

Hyperbolic equations are marginally stable, and in numerical calculations they typically generate unstable oscillations. It is customary to control these oscillations numerically by inclusion of a viscous damping term. Since the inclusion of a new term (or the modification of a coefficient, so that a previously negligible term becomes significant) changes the equation, it must be anticipated that in some cases the resulting change in the equation and its solution is undesirable. As an example, we mention combustion chemistry: a numerical mixing of burned and unburned reagents across the flame front would significantly alter the problem [3, 7]. A second example ocurs in the use of a surfactant as a tertiary recovery agent in petroleum reservoir engineering: numerical dispersion of the surfactant away from a water oil concentration front would again alter the problem [1, 11].

Among the methods which can be used for these problems, we mention: the method of characteristics, mesh refinement, shock-fitting, and the random choice method [4, 2]. The latter method has already been applied to a number of practical situations [1–3, 8, 13], but is not widely understood from a numerical point of view. We analyze tracking methodss (i.e., mesh refinement and shock-fitting) in the context

* Supported in part by NSF Grant PHY-78-08066.
† Supported in part by the Army Research Office, ARO Grant DAAG29-7B-G-0171.
‡ Permanent address: Mathematics Department, Pontificia Universidade Catolica de Rio de Janeiro, Rio de Janeiro, Brazil.
§ Supported in part by NSF Grant DMR 77-04105.
** Permanent address: Mathematics Department, Cornell University, Ithaca, N. Y.



0021-9991/80/120336–19$02.00/0

of the random choice method. We find that the tracking is remarkably simple. For example, in the case of mesh refinement, one additional mesh point is sufficient. The motivation for this work is twofold. First, we want to test methods in one dimension which may be useful in two dimensions, and second, we want to analyze the sources of the errors in the one-dimensional random choice method. This is done by turning the errors off one at a time.

In this paper we consider mainly Burgers' equation

$$u_t + uu_x = 0.$$

Some of our results, reported earlier in [5], indicate that our conclusions based on Burgers' equation extend to the equations of gas dynamics. In the authors' judgment the proposed methods are even more advantageous in the case of contact discontinuities, which are blurred by standard difference schemes. See Section 8, and especially Fig. 10. The posibility of extending these methods to two dimensions is beyond the scope of the present paper, but we can report that an initial phase of this extension (passive tracking) is now operating satisfactorily and will be described in a subsequent publication.

## 2. The Random Choice Method

General references for this method are [9, 10, 14]. In the RC method, the solution at time $t = n\Delta t$ is taken to be piecewice constant on intervals of size $\Delta x$, with discontinuities at $(i + 1/2)\,\Delta x$, i.e.,

$$u^{(\Delta x)}((i + a)\,\Delta x, n\,\Delta t) = U_i^n \qquad \text{for} \quad -\tfrac{1}{2} \leqslant a < \tfrac{1}{2}, \tag{2.1}$$

and for $i = 1, 2,...,$ and for $n = 0, 1,....$ An exact solution can then be given for

$$n\,\Delta t \leqslant t < (n + 1)\,\Delta t. \tag{2.2}$$

In fact, each jump discontinuity gives rise to a Riemann problem [4]. (See Fig. 1.) By definition a Riemann problem is a Cauchy problem for a hyperbolic equation in one dimension, with data that have a single jump discontinuity and are otherwise constant. For a Riemann problem with a jump discontinuity at $x = 0$, the solution is a function of $x/t$. For an $n \times n$ system, the solution will generally consist of $n$ distinct, noninteracting waves, although a more complicated wave structure can result. The Riemann problem can be reduced to a nonlinear functional equation, and it is feasible to solve it numerically, at each mesh point and time step, for a number of problems which have been studied to date. Because of finite propagation speed, any problem with piecewise constant data can be solved for a time interval (as in (2.1)) merely by putting together solutions of Riemann problems. The differential equation, in the form of a nonlinear conservation law,

$$u_t + f(u)_x = 0, \tag{2.3}$$

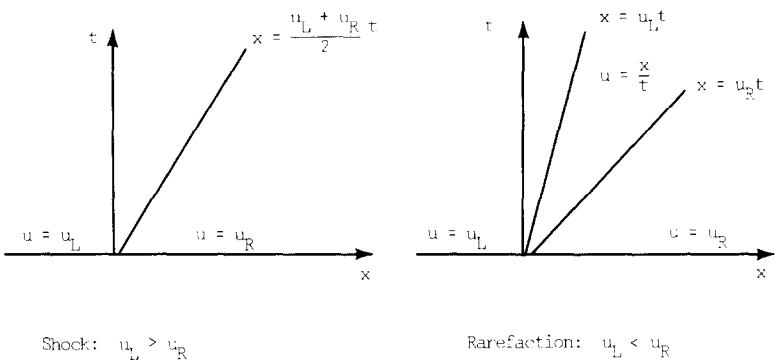


FIG. 1. The Riemann problem for Burgers' equation.

and the associated entropy condition define uniquely the solutions of these Riemann problems. An aproximate solution $u^{(\Delta x)}$ is obtained by this construction,which is now described in detail.

We denote by $\phi(x, t, u_L, u_R)$ the solution of the Riemann problem with Cauchy data at $t = 0$ given by $u = u_L$ for $x < 0$ and $u = u_R$ for $x > 0$. (See Fig. 1.) Given $U_i^n$, $i = 1, 2,...$, we define

$$u^{(\Delta x)}((i + \tfrac{1}{2} + a)\,\Delta x, (n + b)\,\Delta t) = \phi(a\,\Delta x, b\,\Delta t, U_i^n, U_{i+1}^n) \tag{2.4}$$

for

$$\tfrac{1}{2} \leqslant a < \tfrac{1}{2}, \qquad 0 \leqslant b < 1, \qquad i = 1, 2,....$$

This procedure is well defined provided $\Delta t$ is less than $\Delta x/2$ divided by the maximum characteristic speed. Thus $u^{(\Delta x)}$ is not piecewise constant for $t = (l + 1)\,\Delta t - 0$. By a sampling procedure, depending on a sequence $\{\theta_l\}$ equidistributed [9] on $[0, 1]$ we define the new constants

$$U_i^{n+1} = u^{(\Delta x)}(\Delta x(i + \theta_{n+1}), (n + 1)\,\Delta t - 0) \tag{2.5}$$

so that the inductive construction of $u^{(\Delta x)}$ can continue. It is easy to combine (2.4) and (2.5) to obtain the RCM procedure. This version avoids staggered grids and is more convenient for tracking shocks and for multidimensional problems. Sampling means that at each mesh time $t = n\,\Delta t$, $u^{(\Delta x)}$ is forced to be piecewise constant, and the value of this constant (2.5) is determined by sampling the values

$$u(\Delta x)|_t = (n + 1)\,\Delta t - 0.$$

By definition, a sequence of numbers $\{\theta_n\}$, $0 \leqslant \theta_n \leqslant 1$, is equidistributed in $[0,1]$ if for any subinterval $[a, b] \subset [0, 1]$, the fraction of $n$'s (asymptotically for large $n$) with $\theta_n \in [a, b]$ is just $|b - a|$.

The effect of this construction is that the solution is viewed as being composed of elementary waves. Throughout the calculation, each wave preserves its integrity exactly, but its position and velocity are correct only on the average and are subject to random errors.

As long as the wave does not interact with other waves, its motion is a random walk, governed by the equidistributed sequence $\{\theta_n\}$. The more rapidly $\theta_n$ is equidistributed, the smaller are the position errors in the wave. If $P(t)$ denotes the position of the wave at time $t$ and

$$\delta P(t) = P(t)_{\text{computed}} - P(t)_{\text{exact}}$$

is the error in $P(t)$, then theory of equidistributed numbers [6] shows that for $t$ bounded

$$|\delta P(t)| \leqslant O(1)\,\Delta x(|\ln \Delta x| + 1) \tag{2.6}$$

is an optimal bound. No choice of $\theta_n$ can improve on (2.6) for all wave speeds. Further (2.6) is sharp in the sense that it is achieved for some examples of equidistributed sequences $\{\theta_n\}$. In particular, we mention

$$\theta_n = n\sqrt{2} \pmod 1 \tag{2.7}$$

and a Van der Corput sequence for which

$$\theta_n = \cdot\, l_0 l_1 l_2 \ldots \tag{2.8}$$

is a binary number where $n = \ldots l_2 l_1 l_0$ is the binary representation of $n$. Thus the Van der Corput sequence (2.8) is given as

$$\{\theta_n\} = \{\tfrac{1}{2}, \tfrac{1}{4}, \tfrac{3}{4}, \tfrac{1}{8}, \tfrac{5}{8}, \tfrac{3}{8}, \tfrac{7}{8}, \ldots\}.$$

A numerical analysis of $\delta P(t)/\Delta x$ for these $\{\theta_n\}$ and a variety of wave speeds revealed the following behavior. $\delta P(t)/\Delta x$ consists of rapid oscillations, of magnitude between 1 and 2, between slowly varying upper and lower envelopes. The envelopes change slowly with time and somewhat more rapidly with the dimensionless wave speed

$$u_{\text{d}} = u_{\text{dimensionless}} = u\,\Delta t/\Delta x.$$

Note that $|u_{\text{d}}| < \frac{1}{2}$ is the Courant–Friedrichs–Lewy stability condition. For the Van der Corput sequence, the speeds near dyadic rationals are exceptional: for $u_{\text{d}}$ a dyadic rational, $\delta P(t)/\Delta x$ is a periodic function of $t$. Near the small denominator dyadic rationals, $u_{\text{d}} = 0, \pm\frac{1}{2}$, $\delta P(t)/\Delta x$ has an exceptional character. Elsewhere, we found lower and upper envelopes for $\delta P(t)$ with the approximate values 0 and 1.5, respectively, for up to 2000 time steps. Typical plots are shown in Fig. 2a.

The sequence (2.7) has more nearly symmetric envelopes but which cannot be approximated by a time-independent constant; see Fig. 2b.

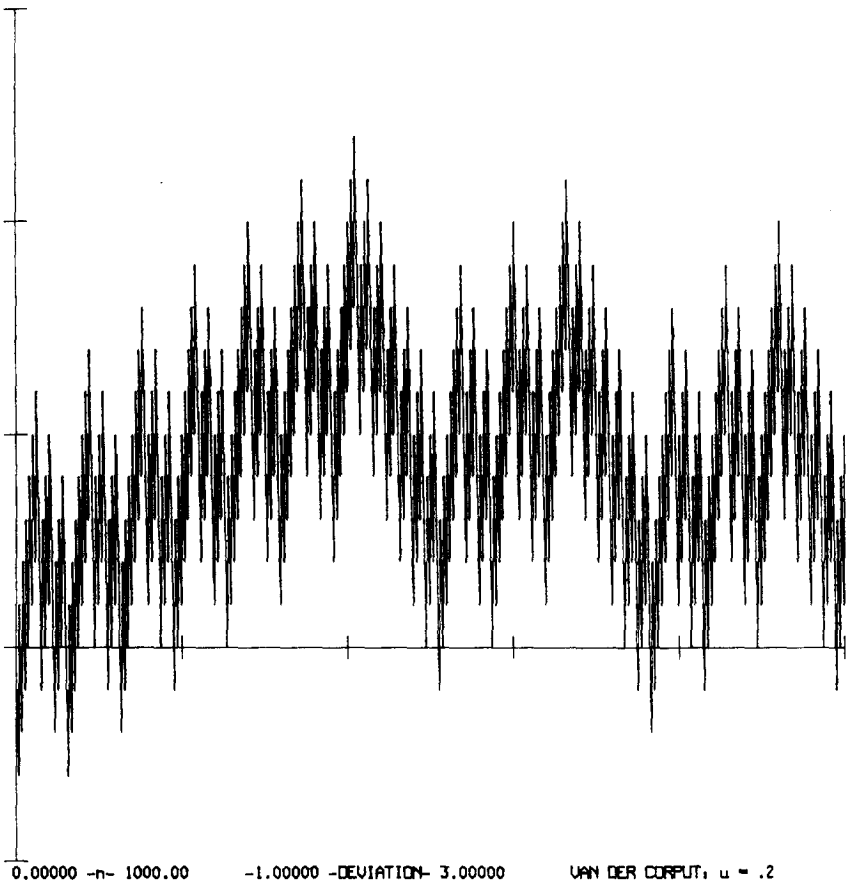


FIG. 2a. Deviation in position of a characteristic curve as a function of $t$, measured in units of $\Delta x$, for the Van der Corput random number generator.

In Fig. 3, we show the Cauchy data used in this paper. The label *abcd* stands for $u(-2) = a$, $u(0) = b, c$, $u(+2) = d$, at time $t = 0$.

## 3. TRACKING I: ONE-POINT MESH REFINEMENT (PCR)

In the random choice method, the primary source of error in the position $P(t)$ of the discontinuity under consideration, of course, is the statistical fluctuations in the position of each wave, as portrayed in Fig. 2. A secondary source of error arises from incorrectly positioned waves of the same family as $P$. Additionally, (a) incorrectly positioned waves of distinct families also contribute to the eror, and finally, (b) there is an error (unrelated to the statistics) resulting from the fact that the speed in $P$ is computed by a first-order accurate Euler ordinary differential equation time step. (b) is the minimum error associated with any first-order scheme, and, for a wave or characteristic moving through an otherwise smooth solution, results from a first-order

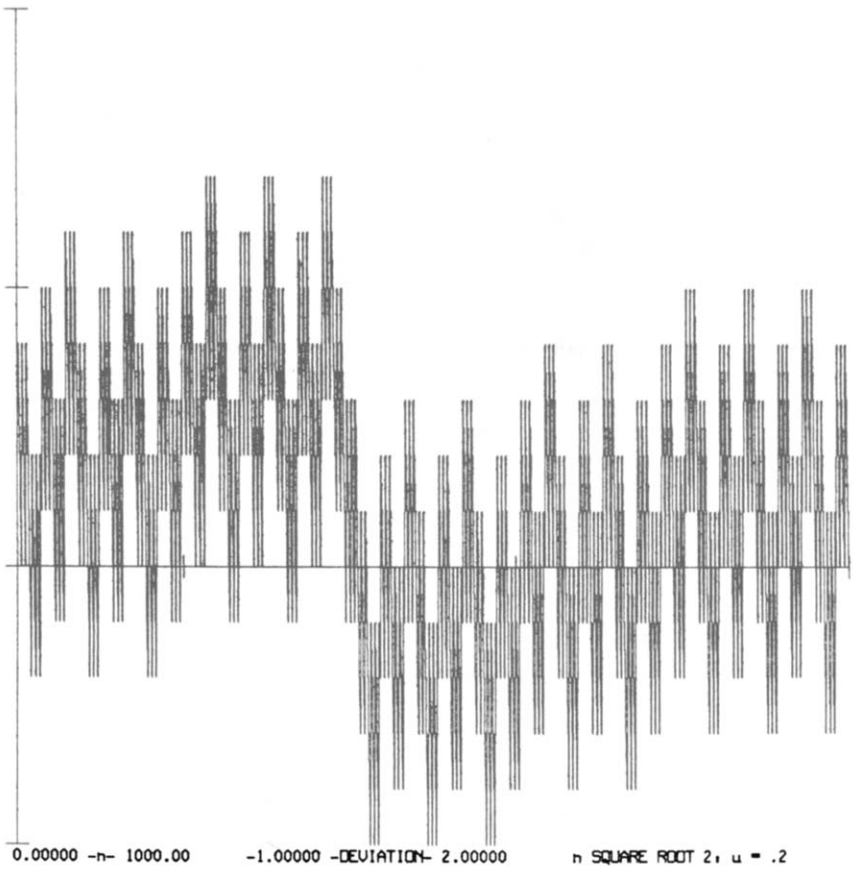


FIG. 2b. Deviation in position of a characteristic curve as a function of $t$, measured in units of $\Delta x$, for the $n\sqrt{2}$ random number generator.

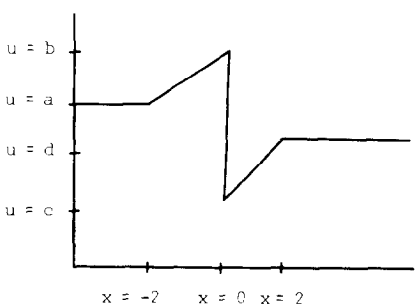


FIG. 3. Cauchy data.

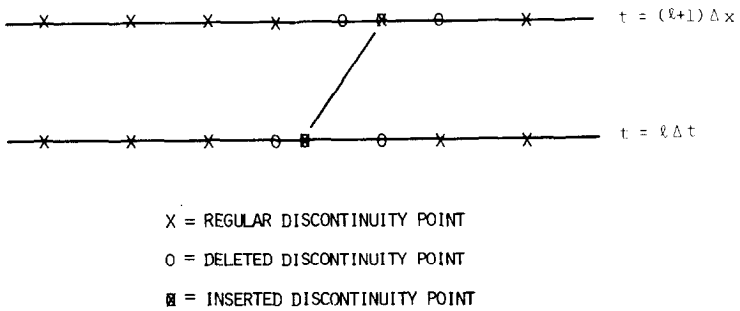


FIG. 4. Mesh refinement used to track a discontinuity.

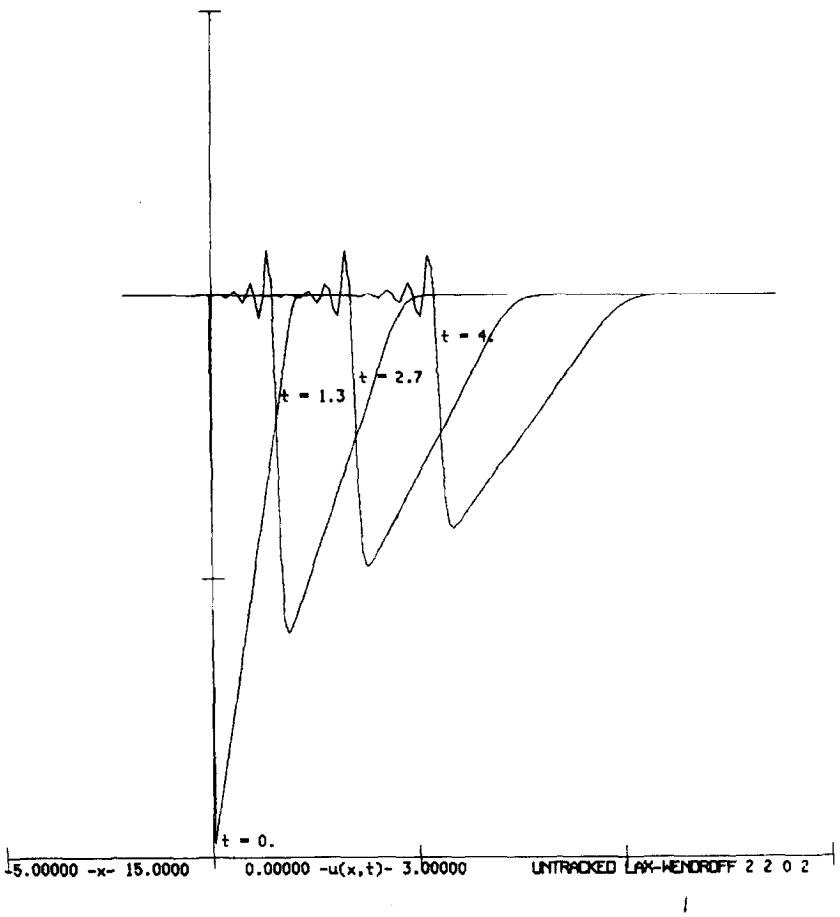


FIG. 5a. $u$ vs. $x$ for the Lax–Wendroff methods.

approximation of the smooth part of the solution by piecewise constant data at each time step. Thus, this error could also be viewed as an aspect of (b) and of the secondary error.

The effect of (a) was analyzed earlier [5] and is smaller than the secondary error. For this reason we do not consider it further, and concentrate on Burgers' equation, which has only one family of waves. The effect of (b) is about $(0.01\Delta x) \cdot T$ in our experiments, i.e., about 20 times smaller than the secondary error. Thus, we concentrate on primary and secondary errors.

The one-point mesh refinement is designed to eliminated only primary errors [5]. A new discontinuity point is introduced at each time step $t = (l+1)\Delta t$, located exactly on the discontinuity in the computed solution (2.5), using one step of a first-order Euler ordinary differential equation scheme. (See Fig. 4.) Prior to the sampling, neighboring discontinuity points are then deleted, to preserve a CFL stability

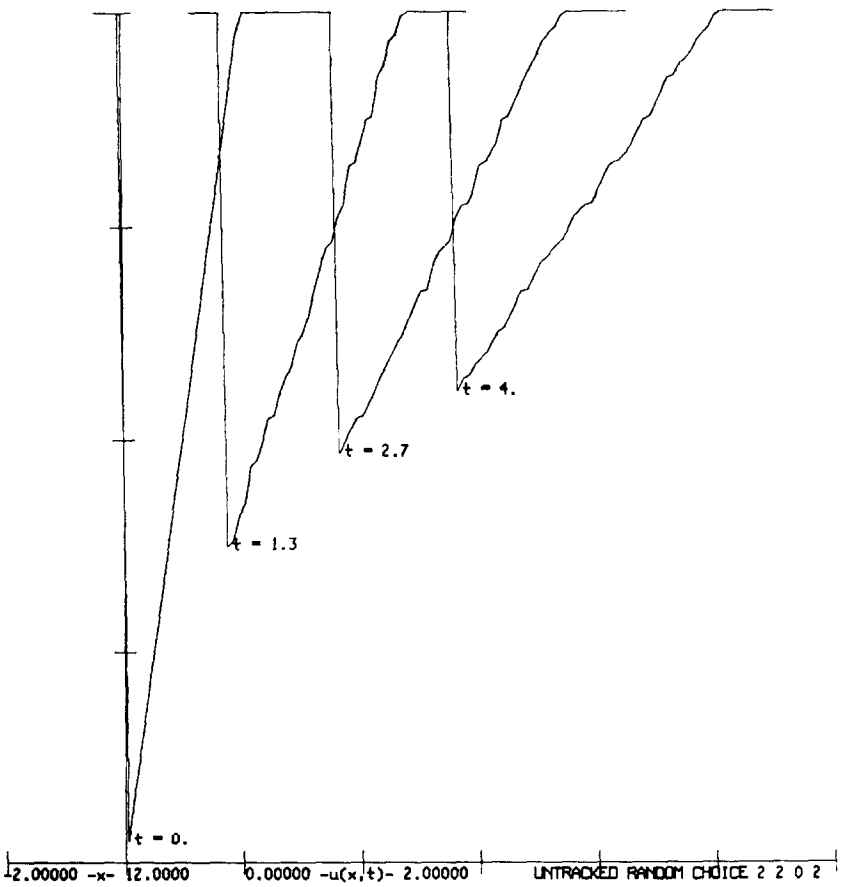


FIG. 5b. $u$ vs. $x$ for the random choice method.

condition for a future time step. The sampling on the two enlarged intervals neighboring the shock is done by stretching linearly in (2.4). The result is that the sampling error in the discontinuity is zero. Thus, we are left only with the secondary error resulting from the interaction of the discontinuity with first-order errors in the positions of the other smaller waves.

In order to implement the one-point mesh refinement, we use a one-step scheme (i.e., the grid is not staggered)) in contrast to [4, 2]. See Fig. 4.

## 4. Tracking I: First-Order Shock-Fitting (TRC)

The solutions of Section 3 contain a systematic first-order error. This error is a stopping time effect, due to position fluctuations in the rarefaction waves with which $P$ is interacting. Because waves of the same family have fairly similar speeds, the approach of these interacting waves is oblique. The stopping time is the time of first interaction of the shock and the rarefaction wave. After this first interaction, the waves coalesce and no longer have a separate identity. Due to the slow approach (about 40 time steps in our problem), the stopping time is governed by the envelope of the rarefaction wave position and is essentially unrelated to rapid fluctuations in the rarefaction wave position. In case the relevant (right or left) envelope is not at zero, all incoming rarefaction waves will have the same sign in their stopping time error (normally they will interact too soon). In other words, because of statistical fluctuations in the speed of the characteristics, the characteristics tend to hit the shock too early. This gives a small, but systematic error in shock speed, never larger than $0.5\Delta x$ per unit time, in the runs we considered.

For the VdC sequence the envelopes appear to be fairly regular, and have a uniform shift, so that the left envelope of the rarefaction wave very nearly coincides with its exact position, while the right envelope is located at a distance perhaps $1.5\Delta x$ to the right of its exact position; cf. Fig. 2.

To test this interpretation of the stopping time errors, we modified the one-point mesh refinement solution to allow a correction for this effect. We chose a very simple correction, which then brought the method close to the shock-fitting of [12]. The idea is to let the solution be multivalued in a small neighborhood of the tracked shock. To simplify the conceptual discussion, we use a pair of functions $u_l(x, t)$ and $u_r(x, t)$, so that the solution is double valued everywhere. Each single-valued function, $u_l$ and $u_r$, is advanced by the ordinary sampling method or by a Eulerian finite difference scheme. In this way, the dynamics which govern $u_l$ aand $u_r$ never see the shock discontinuity. After advancing both $u_l$ and $u_r$ by one time step, the shock position is advanced one time step, as a solution of an ordinary differential equation. With the multivalued solution, it is posible to postpone the shock–rarefaction cancellation, so that in effect it occurs after the rarefaction wave has progressed beyond the shock by a specified distance, determined by the envelope of the random number generator. In other words, the ordinary differential equation which advances the position of the

discontinuity in time is defined by means of the two branches of the double-valued solution. The double-valued solution is evaluated, however, not at the discontinuity position, but at the position corrected for the envelope of the random number generator. The construction, desired here for a single-component equation such as Burgers' equation can be modified for a multi-component equation such as gas dynamics. The initialization of $u_l$ $(x, t = 0)$ and $u_r$ $(x, t = 0)$ is very simple. We define $u_l(u_r)$ to be the Cauchy data at the left (right) of the shock, and we extrapolate it continuously as a constant at the right (left) of the shock. This procedure is adequate for the first-order random choice method with tracking.

## 5. Tracking III: Tracked Lax Wendroff (TLW)

Here we use the (second-order accurate) Richtmeyer version of the Lax Wendroff scheme to advance the time step in each single-valued component $u_l$ and $u_r$ of $u$, and

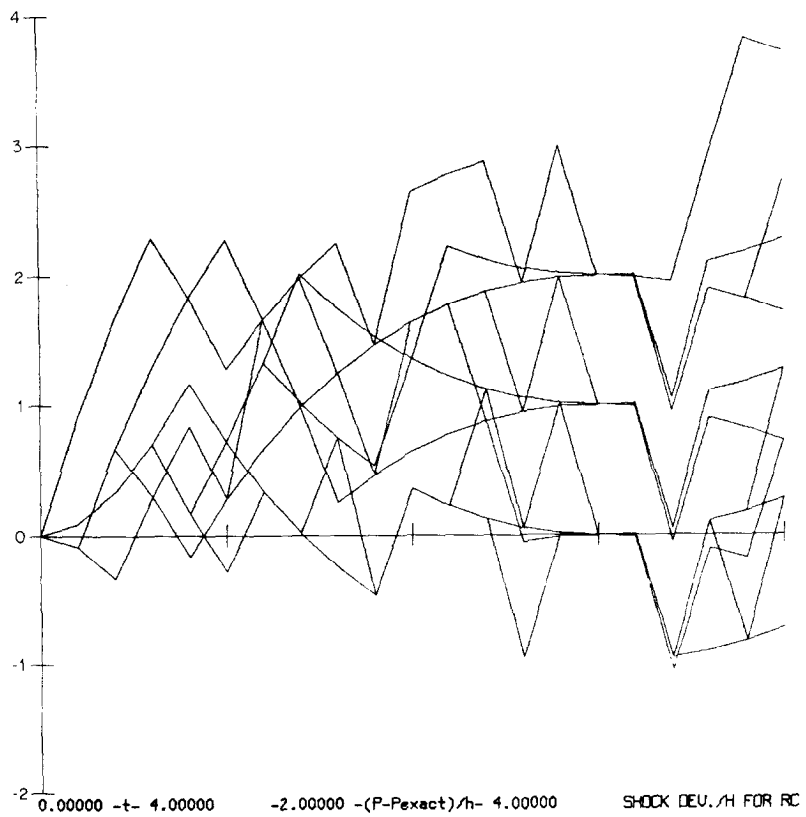


FIG. 6a. $\delta P/h$ vs. $t$ for the random choice solution—14 choices of Cauchy data.

a first-order ODE to advance the shock position. The initialization of $u_l$ and $u_r$ is done as before, except that the extrapolation to the unphysical region required matching at least first derivatives (first-order extrapolation).

The position of the shock obtained in this way is identical to the one obtained by solving the ODE using the analytic solution which can easily be computed for our Cauchy data. This indicates that all PDE errors have become negligible: in fact, now $\delta P \cong (0.01\Delta x)\, T$.

We emphasize as essential two features of the methods for tracking I, II: the zeroth-order (i.e., continuous) double-valued extrapolation of the solution and subsequent location of the discontinuity by the method of characteristics. We intend to test these methods in two-dimensional calculations. The zeroth-order extrapolation of the first-order tracking is elementary. Since a discontinuous derivative in the solution does not cause a numerical instability in RCM, the extrapolation need only be continuous. In one dimension, extrapolation by a constant is sufficient. Thus, adap-

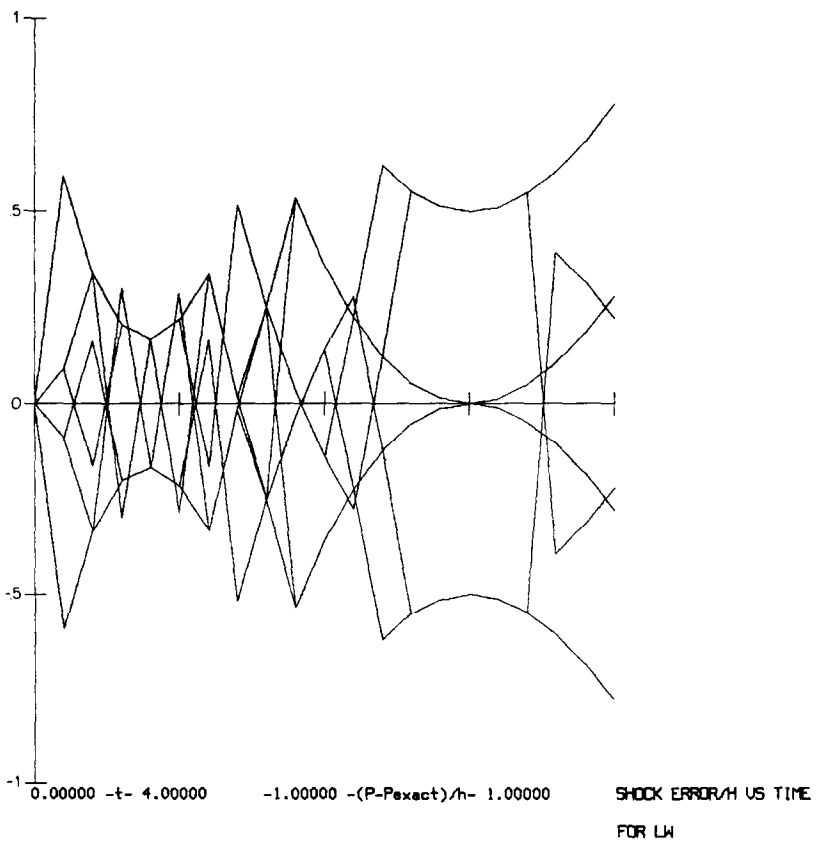


FIG. 6b. $\delta P/h$ vs. $t$ for the Lax–Wendroff solution—14 choices of Cauchy data.

tation to more complicated equations, such as gas dynamics, causes no additional problems. (See Section 8.) The extrapolation for second-order tracking should have continuous first derivatives. We have not determined whether this is practical for more complicated problems.

## 6. Standard Finite Difference Scheme

For comparison with the other schemes, we used the Richtmeyer two-step version of the Lax–Wendroff scheme, with nonlinear viscosity. The viscosity was so small that it did not eliminate completely the overshoots at the shock. To define the spread, we first located the right and left edges of the shock region, defined so that, for example, at the upper edge of the shock, $u$ takes a value which is within 97% of its peak, as measured from the low point. The spread is the distance between the edges, and we located the shock position as the midpoint of the edges.

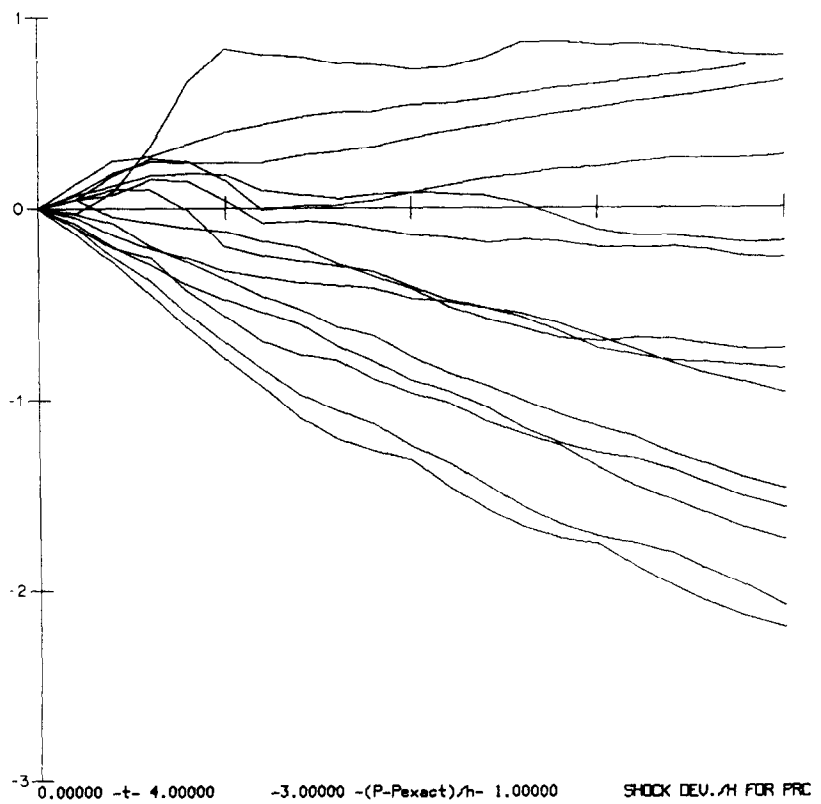


FIG. 6c. $\delta P/h$ vs. $t$ for the one-point mesh refinement—14 choices of Cauchy data.

## 7. Comparison of Results

We solve Burgers' equation by five methods, with 14 choices of Cauchy data, each consisting of a shock of height 2 facing a rarefaction wave of unit strength. The time interval is $0 \leqslant t \leqslant T = 4$. We chose $h = \Delta x = 0.1$ and $k = \Delta t = 0.0133$. See [5] for the effect of mesh refinement.

In Fig. 5, we plot the solution as a function of $x$, for four selected times, for the Lax–Wendroff and random choice methods.

In Table I, we summarize the results by comparing worst case data for five methods. Because of the one-sided bias of the Van der Corput generator, the worst case PRC results are not as good as the $n\sqrt{2}$PRC results reported earlier [5]. The plot of $\delta P/\Delta x$ vs time is given in Figs. 6a–e for five methods. These plots are not graphs of solutions, but represent errors, normalized by division by mesh length. Thus they are the coefficients of $\Delta x$ in a first-order estimate of the form

$$\text{error} \leqslant O(1)\,\Delta x.$$

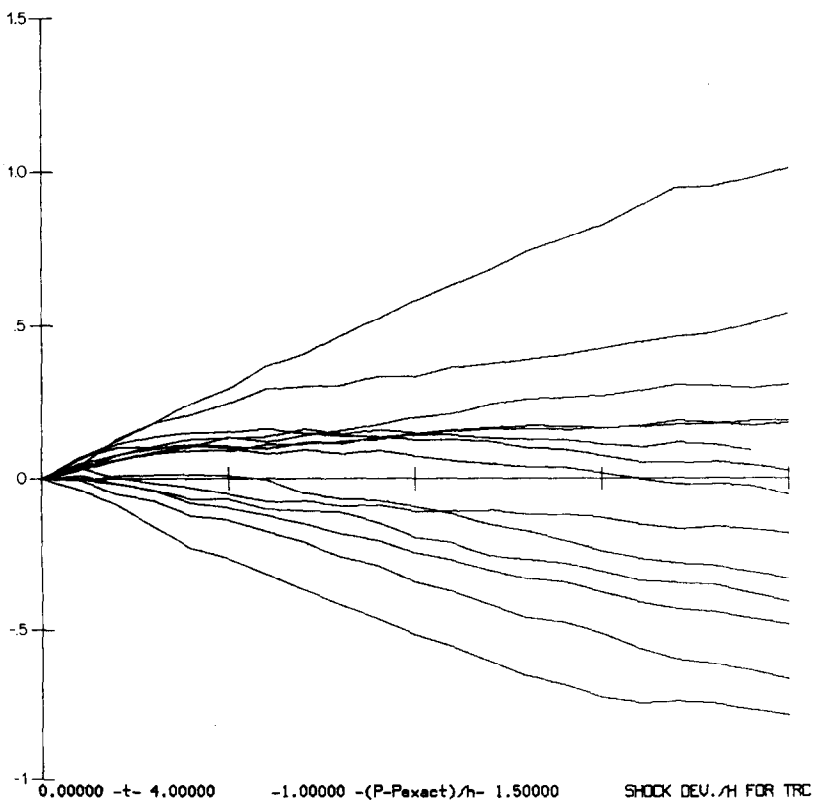


FIG. 6d. $\delta P/h$ vs. $t$ for the first-order shock-fitting—14 choices of Cauchy data.

TABLE I

Comparison of Worst Case Data for Five Methods

| Method | Defined in | Spread | Accuracy | |
|---|---|---|---|---|
| | | | $\lvert\delta P(t=1)\rvert$ | $\lvert\delta P(t=4)\rvert$ |
| LW | Section 6 | $5\,\Delta x$ | $0.3\,\Delta x$ | $0.8\,\Delta x$ |
| RC | Section 2 | 0 | $2.3\,\Delta x$ | $3.7\,\Delta x$ |
| PRC | Section 3 | 0 | $0.8\,\Delta x$ | $2.2\,\Delta x$ |
| TRC | Section 4 | 0 | $0.3\,\Delta x$ | $\Delta x$ |
| TLW | Section 5 | 0 | $0.025\,\Delta x$ | $0.06\,\Delta x$ |

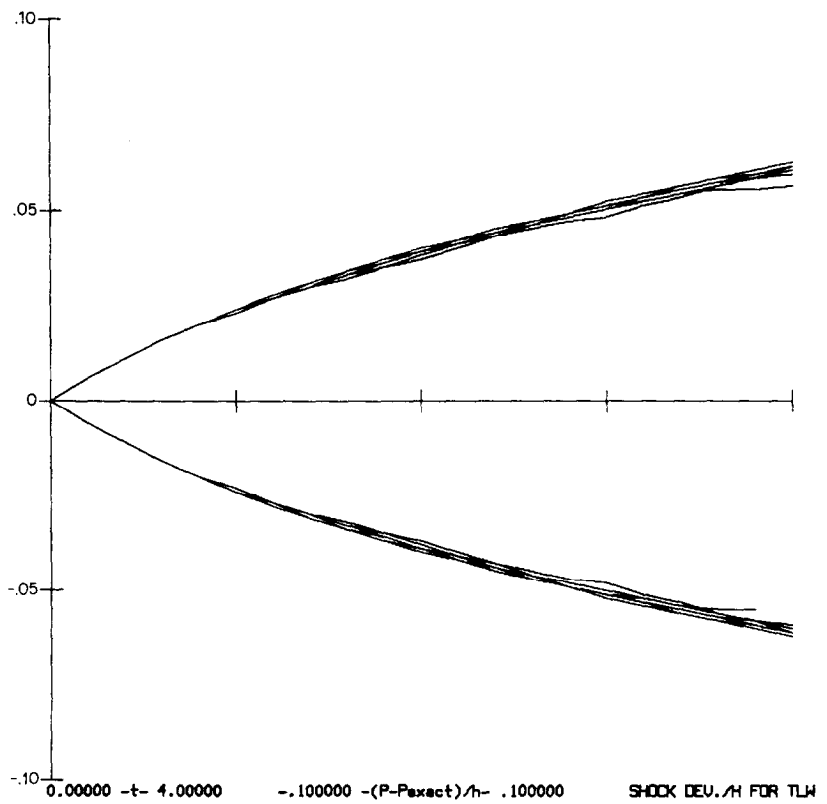


FIG. 6e. $\delta P/h$ vs. $t$ for tracked Lax–Wendroff—14 choices of Cauchy data.

The main information from these graphs is already contained in Table I, and the graphs are included only as supporting evidence.

Note that the scale of the vertical axis is not the same within these five graphs. The plotting time was every 30 time steps. Plotting every time step would introduce more fluctuations into the RC and LW plots, but not otherwise effect the appearance of the graphs. The definition chosen for shock position in LW is constrained to be an integer or half-integer multiple of a mesh point, which accounts for the lack of smoothness in these plots. The RC plots fluctuate because of the statistics inherent to the methods. In Figs. 7a and b, we compare five methods for fixed choices of Cauchy data. In Fig. 8, we plot shock position vs. time for all five methods. Note that the fluctuating RC shock position stays within the LW upper and lower limits. All tracking methods give good results and are too close to the exact solution to be labeled. All tracking methods have perfect resolution and good accuracy. Neither tracking nor the random choice method introduce programming complexities. At least

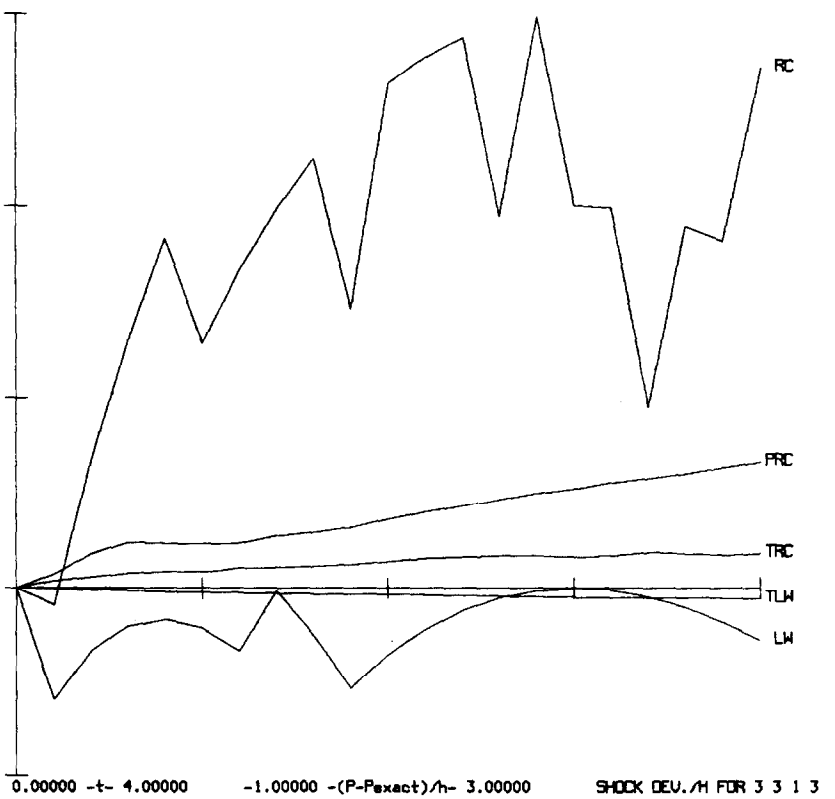


FIG. 7a. $\delta P/h$ vs. $t$ for five methods and one choice of data.

for first-order tracking (zeroth-order extrapolation), extension to more complicated problems may be practical.

## 8. Gas Dynamics

In this section, we summarize and extend results reported earlier [5]. We solved the one-dimensional equations of gas dynamics for isentropic flow of an ideal gas with $\gamma = 1.4$. We used both the RC method (Section 2) and the PRC method (Section 3), for the following Cauchy data: velocity $= -10^2$ m/sec, constant density ($-5$ kg/m$^3$) and pressure with a jump discontinuity from $5 \times 10^5$ to $1 \times 10^5$ N/m$^2$. We tracked either the shock or the contact discontinuity. The results were so similar to the ones for Burgers' equation that the authors decided to use only the later equation to make complete comparisons of the different methods.

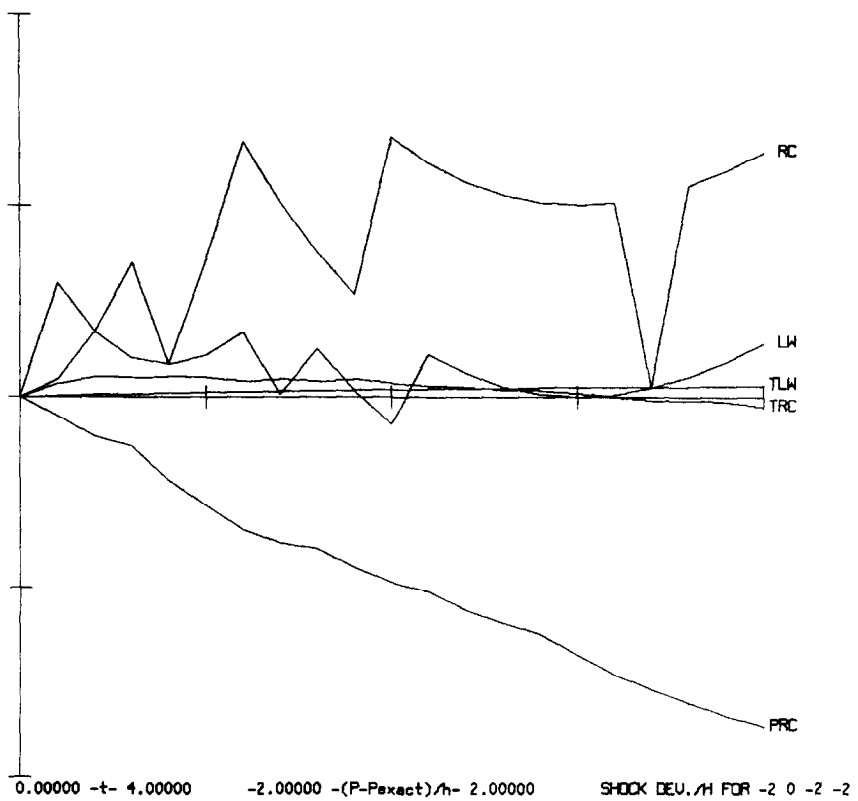


FIG. 7b. $\delta P/h$ vs. $t$ for five methods and a second choice of Cauchy data.

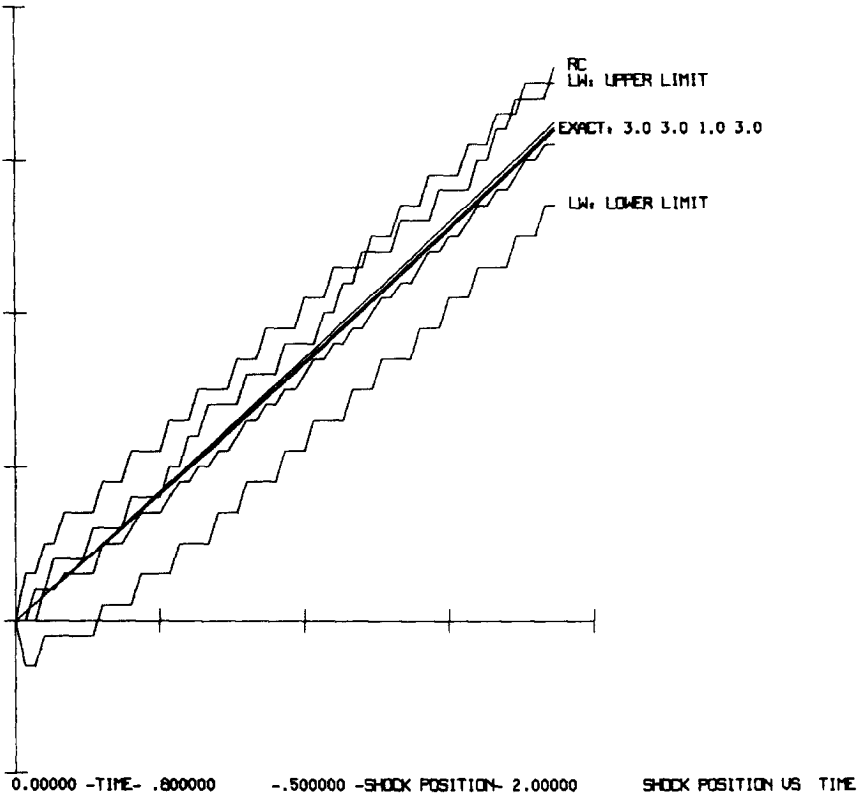


FIG. 8. Shock position vs. time for five methods.

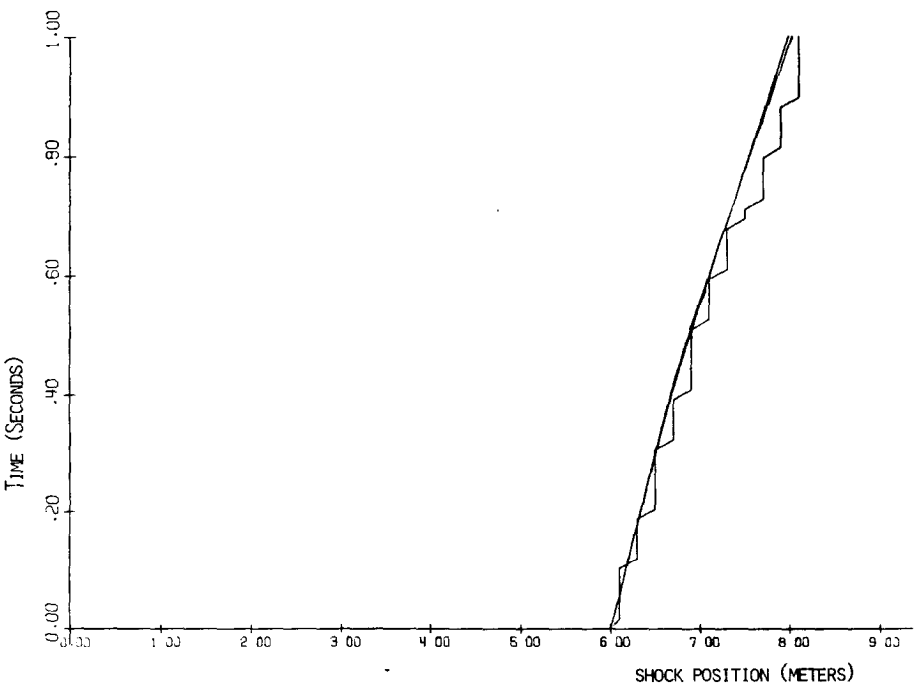


FIG. 9. Shock position vs. time in gas dynamics, for the untracked (RC) and tracked (PRC) methods.

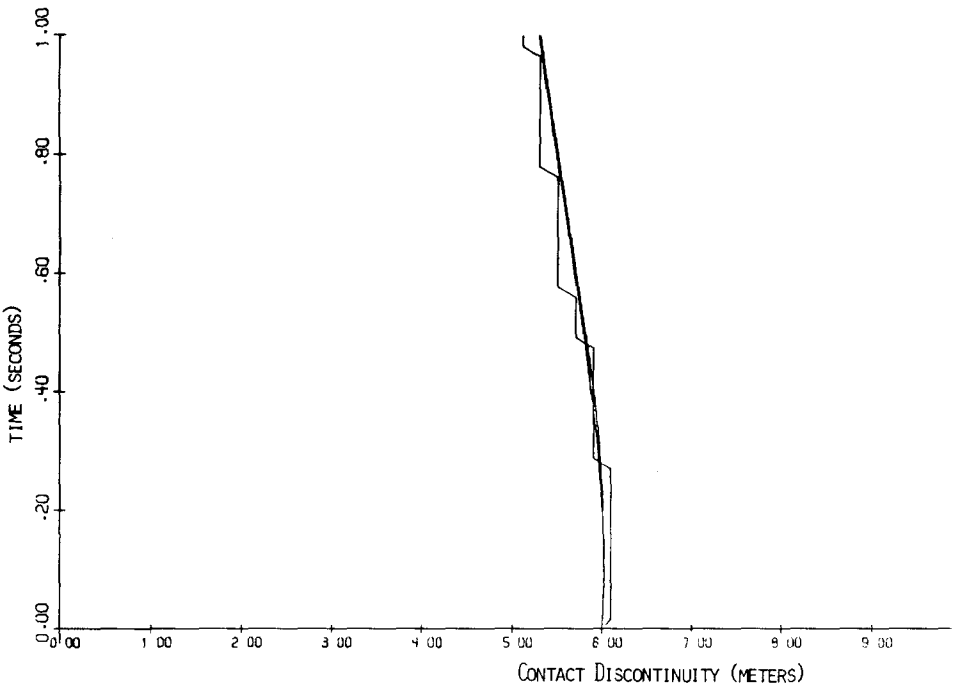


FIG. 10. Contact position vs. time in gas dynamics, for the untracked (RC) and tracked (PRC) methods.

We have plotted the position of the discontinuity $P(t)$ vs. $t$ for both tracked and untracked methods, and for the exact solution. The discontinuity is a shock in Fig. 9 and a contact discontinuity in Fig. 10. In both figures the tracked solution coincides with the exact solution, within the accuracy of the plot. Since an analytic solution was not available, the numerical solution obtained from a much finer mesh was considered as the exact solution.

## REFERENCES

1. N. ALBRIGHT, P. CONCUS, AND W. PROSKUROWSKI, "Numerical Solution of the Multidimensional Buckley–Leverett Equation by a Sampling Method," presented at the Society of petroleum Engineers 5th Symposium on Reservoir Simulation, Denver, Colorado, 1979.
2. A. CHORIN, *J. Computational Phys.* **22** (1976), 517.
3. A. CHORIN, "Flame advection and propagation algorithms," Berkeley preprint, 1979.
4. J. GLIMM, *Commun. Pure Appl. Math.* **18** (1965), 697.
5. J. GLIMM AND D. MARCHESIN, "Subgrid Resolution of Fluid Discontinuities," presented at the ARO Conference on Numerical Analysis, El Paso, Texas, 1978.
6. L. KUIPERS AND H. NIEDERREITER, "Uniform Distribution of Sequences," Wiley, New York, 1974.
7. P. D. LAX, "Hyperbolic Systems of Conservation Laws and the Mathematical Theory of Shock Waves," Monograph No. 11, SIAM Conference Board of the Mathematical Science, 1973.

8. S. LIN, Thesis, University of California, Berkeley, Calif.
9a. P. D. LAX, *SIAM Rev.* **2** (1979), 7.
9b. T.–P. LIU, *Commun. Math. Phys.* **57** (1977), 135.
10. C. MORAWETZ, *Bull. Amer. Math. Soc.*, to appear.
11. G. POPE, "The Application of Fractional Flow Theory to Enhanced Oil Recovery," Society of Petroleum Engineers Paper #7660.
12. R. RICHTMEYER AND K. MORTON, "Difference Methods for Initial Value Problems," Interscience, New York, 1957.
13. G. SOD, "Automotive Engine Modeling with a Hybrid Random Choice Method," Society of Automotive Engineers, Technical Paper 790242.
14. P. COLLELA, Ph. D. thesis, University of California, Berkeley, Calif., 1979.